PARAGENETIC HISTORY OF MULTIPLE MINERAL PHASES IN OOIDS FROM GREAT SALT LAKE, UT

By:
Tyler Lincoln
Geological Sciences, University of Colorado at Boulder

April 1, 2020

Thesis Advisor:
Lizzy Trower
Department of Geological Sciences

Defense Committee:

Lizzy Trower,
Department of Geological Sciences

Brian Hynek
Department of Geological Sciences

Jeffrey C. Cameron
Department of Biochemistry

ABSTRACT

The shallow saline waters of the Great Salt Lake (GSL), Utah are host to modern ooid sand. Ooids here consist of a nucleus particle surrounded by layers of aragonite and other minerals. The cortical fabrics include from radial, concentric, or a combination of the two. Mapping of ooids sampled from multiple sites around the lake revealed distinct areas of an amorphous magnesium silicate phase amongst the aragonite. This study aims to reveal the paragenetic history of co-occurring minerals within the ooid cortices. Understanding the mineralogic sequencing in ooid fabrics can help begin to resolve questions regarding the necessary conditions for ooid formation and growth and may serve as proxies for ooids found in stratigraphic record. Transmitted light microscopy, element mapping with electron microprobe, scanning electron microscopy (SEM), and synchrotron x-ray fluorescence (XRF) mapping and sulfur K-edge absorption spectroscopy (XAS) were used to determine the spatial relationships between the mineral phases. Large euhedral aragonite crystals were found to cut into Mg-silicate mineral phases and unconformably traverse laminar stratigraphy. XRF image maps confirmed Mg-silicate zones were found to coincide with elemental sulfur (S_0), an intermediate produce from sulfate reducing bacteria. The Mg- silicate phase was not observed in ancient Eocene aged oolite samples from the Green River Formation that share similar cortical fabrics to modern GSL, however, reduced sulfate was found preserved in the grain fabric.

INTRODUCTION

Ooids are sedimentary grains of concentrically coated carbonate that are associated with hypersaline lake and shallow marine environments. Throughout Earth's history, ooids are found both as modern loose sand, and cemented together as oolites within stratigraphic record. The oldest known oolite dates back to the Neoarchean (~2800-2500 mya), found in Boomplaas Formation of Campbellrand Platform of South Africa (Beukes 1983). Studying modern ooid cortical fabrics and their composition provide information about the mechanisms and conditions that control formation, potentially serving as powerful paleoenvironmental proxies.

Geologic Setting

The shallow saline waters of the Great Salt Lake (GSL) in Utah, USA are host to abundant ooid sand deposits. Today, ooid deposits form the many beaches that surround the lake, extending from the shoreline to many meters into the photic zone (Eardley, 1938). The GSL is a remnant endorheic lake of the larger Pleistocene aged lacustrine complex, Lake Bonneville (Eardley, 1938; Spencer et al., 1984; Jones et al., 2009; McGuire, 2014). Inflow for the closed basin is fed by the Jordan, Bear and Weber rivers, as well as some minor groundwater inflow; while the only means of outflow is evaporation. (Jones, 2009). In the Pilot Valley near the western border of Utah and Nevada, deposits of ooids have been found in buried core from the paleo-shoreline of Lake Bonneville (Rey, 2012; McGuire, 2014), indicating that ooid formation has occurred during various stages over the lake's history. Ooids from the modern GSL shoreline at Bridger Bay and Spiral Jetty were dated using ^{14}C isotopes, which indicated that ooids have been accumulating over the last 6000-9000 years (McGuire, 2014; Paradis et al., 2017).

FIG. 1—Overview map of the Great Salt Lake (GSL) and the modern GSL ooid sample locations at Bridger Bay on Antelope Island.

Background and Description of GSL Ooids

GSL ooid sand grains occur unimodally in size, with median grain size measuring ~300 microns in diameter (Trower et al., 2019). The exteriors are smooth, and in many instances mottled with slight concavities. The cortices are defined by concentric layers that precipitate from lake water around a nucleus. Broadly, ooids nucleate indiscriminately on available particles from the environment; at the GSL the ooid nuclei are largely composed of subangular quartz grains and brine shrimp fecal pellets.

Previous petrographic examination of modern GSL ooids has revealed that the cortical fabrics vary among grains, as samples contain light colored, semi-translucent radial banding, fine concentric layers, and/or a combination of the two. Eardley (1938) erroneously concluded that >90% of the radial grain structure was composed of calcite ($CaCO_3$). Later investigators (Kahle, 1974; Sandburg, 1975) used scanning electron microscopy (SEM), electron microprobe analysis, and acid etching to determine that the bulk composition of the grains is the less stable form of calcium carbonate, aragonite. Aragonite manifests in GSL ooids as euhedral needlelike crystals that are variable in size and arrangement, both radially and tangentially (see Figure 2-A) (Sandberg, 1975). Per Eardley (1938), the remaining 10% of the grain composition consisted of anhedral darker colored material. This material appears irregularly, interspersed throughout ooid cortices, and historically has been interpreted as dolomite ($CaMg(CO_3)_2$), and intermeshed micrite and/or hydrated sepiolite clays ($Mg_4Si_6O_{15}$ $(OH)_2 \cdot 6H_2O$) (Eardley 1938; Kahle, 1975; Sandberg, 1975; MacGuire, 2014). (see Figure 2-A). A more recent study of GSL microbialites concluded that these zones that were once interpreted as clay minerals are an amorphous Mg-silicate phase (Pace et al., 2016).

Textural Comparisons

Recent studies on the ooid growth suggest that the uniformity in grain size is a result of a dynamic history of abrasion and precipitation (Trower et al., 2017; 2018). Angular unconformities observed as truncations in the cortical layers of some GSL ooids confirm the succession of abrasion and regrowth (Kahle, 1974). The internal fabrics of the GSL ooids are dissimilar to counterparts from modern shallow marine settings. Ooids belonging to carbonate platforms, such as those from the Caribbean and the Persian Gulf lack the radial banding observed in GSL (Kahle, 1974; Bathurst, 1975; Medwedeff & Wilkinson,1983). Marine grains predominantly exhibit tangential banding fabrics. Dissimilarity in cortical textures between lacustrine and marine ooids may reflect the energy of the host environment (Richter, 1983). Ooids in marine locations may experience frequent agitation and abrasion, as well as intense energetic events such as hurricanes. This frequent agitation and abrasion are thought to hinder the development of radial fabric in grain cortices. In contrast, lacustrine ooids may experience motion and abrasion, but not to the same extent as the marine counterpart (Trower et al., 2018; 2019).

Alternatively, it has been observed that some ancient ooids similarly share radial cortical fabrics to modern GSL grains. Ooids in ancient marine limestones regularly are composed of calcite (Kahle, 1974; Sandberg, 1975). Radial calcite fabric textures are considered to form via diagenetic transformations in ancient marine ooids (Kahle, 1974). Concentrically arranged aragonite crystals are found as relic structures within the cortex fabric (Sandberg, 1975), suggesting that this mineral replacement, also known as neomorphism, here aragonite to calcite is part of the diagenetic process.

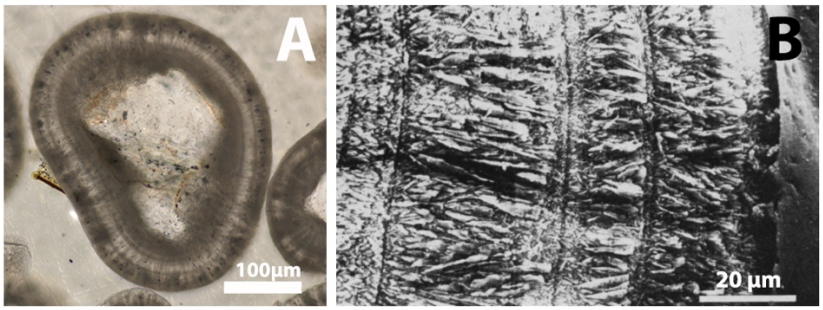

FIG. 2—**A)** Transmitted light microscope image of GSL ooid with a subangular quartz grain nucleus. Aragonite makes up the radial banding and tangential lamination that make up the cortex. **B)** SEM image (Sandberg 1975) of an acid etched portion of a GSL ooid displaying variably oriented aragonite crystal assemblages

Ooid Genesis and Growth

The mechanisms that govern ooid genesis and growth continue to be a contentious topic in carbonate sedimentology and geobiology. Investigations aim to determine whether ooid grain formation corresponds to abiotic, physiochemical factors or whether the accretion process is biologically mediated from lacustrine microbial activity. Early ideas suggested that GSL ooid genesis and growth (Eardley, 1938) was a physical process, stemming from the supersaturation of $CaCO_3$ minerals via the evaporation of brine lakewater. The mineralogic transformations in GSL ooid cortical fabrics have been largely observed and compared to marine analogs (Kahle, 1974; Sandberg, 1975; Trower et al., 2017), but the basis for these changes has been poorly understood.

Sandberg (1975) suggested that the development of aragonite radial bands is a product of depositional processes, opposing diagenetic origins. Later research may provide a link that microbial activity may play a role in the diagenesis and development of certain carbonates including freshwater stromatolites and travertines (Love & Chafetz, 1988; Chafetz & Buczynski, 1992; Freytet & Verrecchia, 1999; Wright, 2019). Scarce literature exists linking similar phenomena to the internal stratigraphy of ooids.

A recent study provided a conceptual outline for the mineralization of GSL microbial mats and may parallel the processes that regulate ooid formation (Pace et al., 2016). Ooids provide a binding substrate for the lithification of microbialites (see figure 3-B) and are commonly found as adjacent facies in stratigraphic records. The study mechanistically outlines a three-part mineralization sequence. 1) First, in hypersaline environments, microbialites begin formation from biofilms created by cyanobacteria. Cyanobacteria are photosynthetic autotrophs, distributed within the photic zone at lakeshore margins. The cyanobacteria here create extracellular organic material (EOM), and oxygenate the local lake water, causing an increase in pH in surface waters. The alkaline lake water provides the favorable conditions for the precipitation of amorphous Mg silicate, considered as a likely precursor to Mg/Si and Ca/Mg bearing minerals, sepiolite ($Mg_4Si_6O_{15}$ $(OH)_2 \cdot 6H_2O$) and stevensite ($(Ca,Na)_xMg_{3-x}(Si_4O_{10})(OH)_2$). X-ray diffraction (XRD) analysis on carbonates from lake sediment cores revealed that as the Bonneville basin has contracted over the 30,000 years, the Mg/Ca ratio has increased. Upon the increase of magnesium concentration with diminishing lake volume, the preferential mode of carbonate precipitation shifted from calcite to aragonite (~12,000-years BP) (Spencer 1984; Jones 2009; Deocampo, 2010). Today, the GSL is fed by Mg^{2+} ions primarily from the Bear River tributary. Dissolved mafic minerals are supplied to the lake as the river flows through a basaltic unit in the Oneida Narrows (Cooley & Pederson, 2012). The current Mg concentration in the GSL is ~170 mmol, over three times the concentration found in seawater, at 50 mmol (Ingalls et al., in press).
Silica is considered to be sourced from lake water but also from dissolution of diatom frustules. 2) Next, aragonite nucleates in areas populated by heterotrophic sulfate reducing bacteria, which decompose EOM and cyanobacteria. Euhedral needle-like aragonite crystals were observed intruding into zones of Mg-silicate. 3) Finally the observance of dolomite ($CaMg(CO_3)_2$) is thought to partially replace aragonite from within neutral/slightly acidic pore water as a tertiary step in the mineralization of the microbial mats.

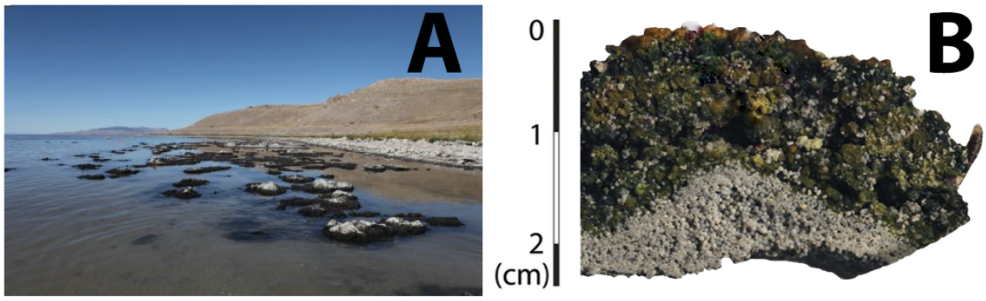

FIG. 3—Great Salt Lake ooid and microbialite facies: **A)** Partially submerged microbialite columns at the GSL shoreline (image from Bouton et. al 2016); ooid sand provided a binding substrate. Grey superficial portions have undergone lithification. **B)** Facies interface between microbial mats and ooids (image from Pace et. al 2016).

Paleoenvironmental Context

The Green River Formation (54–43 Ma) of southwestern Wyoming, northwestern Colorado and northeastern Utah (see figure 4 A-) is one of the most extensively studied paleo-lacustrine systems (Roehler, 1993). The Great Salt Lake, and the geologically recent lake Bonneville can provide the best operative modern analog to this paleoenvironment to search for similar paragenetic mineral phases, as both oolite and fossil microbialite facies are found within Green River Formation stratigraphy. Stacked strata here reveal that over the 9 Ma span of the Green River lacustrine complex, the system underwent a gradational cycle from being an overfilled freshwater basin, to a balanced filled saline lakes, to underfilled hypersaline lake /dry playas, and back to an overfilled freshwater basin (Carroll & Bohacs, 1999). Similarly, the early stages of Bonneville basin underwent cyclical series of filling and underfilling, but since the catastrophic Bonneville Flood at ~14,000 year BP, when the basin waters breached the ancient spillway at Red Rock Pass, Idaho, the basin has been in a regressive stage until present day (Spencer, 1985; Jones, 2009).

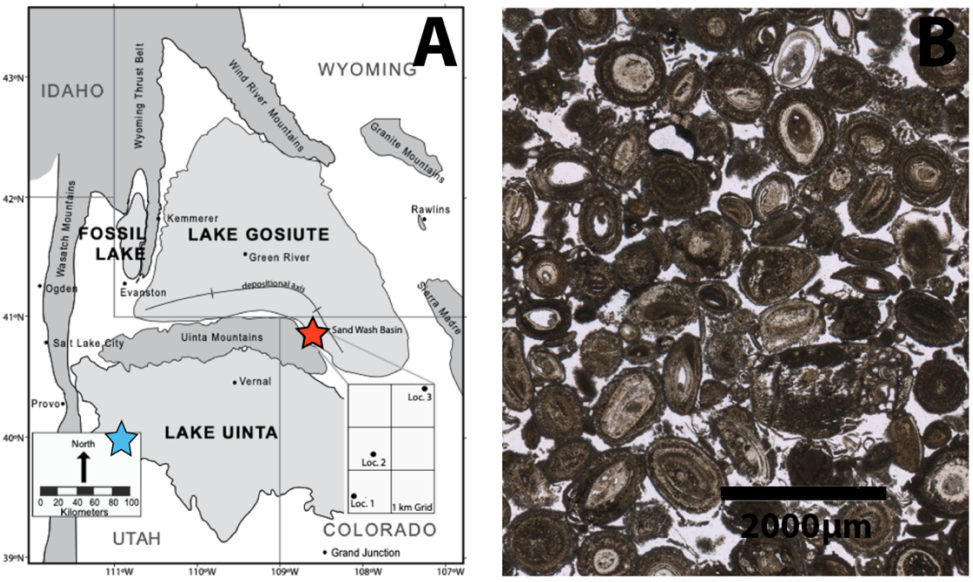

FIG. 4—**A)** Modified map from (Awramik 2015) The red star designates oolite sample location in the Sand Wash Basin. The Blue star designates the Sanpete Valley; the location of stevensite ooids described by Tettenhorst (1978). **B)** Microscope image using transmitted light of Eocene aged oolite from the LaClede bed found in the Sand Wash Basin of the Green River formation with concentric and radial fabric.

Oolite containing Mg/Si has been reported in the Green River Formation. Tettenhorst (1978) observed brown, shiny oolite from the Sanpete Valley in central Utah (see figure 4-A), belonging to a paleo-lake Uinta in the Green River lacustrine province. The composition of the oolite here was determined to largely be Stevensite ($(Ca,Na)_xMg_{3-x}(Si_4O_{10})(OH)_2$), and is abundant in pure mineral form in this location. Stevensite, is a tri-octahedral Mg-silicate that requires waters with a pH >9 and is indicative of precipitation from magnesium-rich waters (Jones, 1986; Wright, 2012). Oolite from another locality in the Green River Formation was selected for this study. The LaClede bed of the Laney Member of the Green River Formation in the Sand Wash Basin is home to the world's largest fossil lacustrine stromatolites (up to 5.5 meters in height), and presumed to have

formed during the saline balanced fill phase of the lacustrine province, along the shores of the paleo-Lake Gosuite (See figure 4-A). Here, akin to the modern GSL, oolite facies are found underlying and surrounding the fossil microbialite deposits. Oolite sampled from the Sand Wash location not only bears resemblance to grains described by Tettenhorst (1978), alike modern GSL ooids, this sample also contains grains displaying both radial and concentric cortex fabrics (see figure 4-B).

Rational for this Project

Since similar mineral assemblages of aragonite and Mg-silicate (Eardley, 1938; Kahle, 1974; Sandberg 1975) are found both within modern GSL ooid cortices and GSL microbialite facies, the neomorphism in GSL ooids may correspond to the 3-part paragenesis model proposed by (Pace et al., 2016). In the lacustrine setting, Mg-silicates have been described to be the host site for bacterial interaction that mediates the precipitation of calcium carbonate. This study uses multiple methods of microscopy and element analysis to determine the mineralization sequencing from modern ooids at the GSL and with that, create a search image template for similar processes in paleo-lacustrine settings.

MATERIALS & METHODS

Optical Transmitted Light Microscopy, Scanning Electron Microscope (SEM) and Electron Microprobe Microscopy

Modern GSL ooid samples were collected at Bridger Bay on the northern end of Antelope Island. The S7 sample was collected at the south end of GSL (see figure 1). GPS coordinates were collected from each of the sample locations of modern ooids and were digitally cataloged using[1] System for Earth Sample Registration (SESAR). Loose ooid grains from samples GSL001-3, BB1, BB5 and S7 were fixed in into epoxy, polished and mounted on thin section slides by Spectrum Petrographics (GSL001, GSL002, GSL003) and High Mesa Petrographics (BB1, BB5, S7). Sample VC-18-24 was collected from the Laney member of the Green River Formation in the Sand Wash Basin of northwestern Colorado (see Figure 4-A) as part of a larger stratigraphic sampling initiative under BLM Paleontological Resources Use Permit COC 078834. Sample VC-18-24 was prepared as a polished thin section slide by Spectrum Petrographics. Each thin section slide was first examined using a transmitted light microscope (Zeiss Axio Imager), in tandem with ZEN software to create mosaic images for navigable maps using a 5x objective. Individual ooid grains were imaged using the z-stack function with a 20x objective.

Electron microscopy was conducted using the JEOL-8230 electron microprobe at the University of Colorado Electron Microprobe Laboratory on July 18, 2019 and January 29, 2020. Samples were carbon coated, and imaged using an accelerating voltage at 15 keV, with a beam current of 17.6 nA. Targeted elements included: Si, Mg, Mn, Fe, Ca. A total of 22 sites were mapped from Bridger Bay samples, and 6 grain sites were mapped from the S7 locality.

[1]Geo-sample GPS coordinate repository SESAR: https://www.geosamples.org/

Thin section slides were carbon coated in preparation for SEM imaging. Backscattered electron images were collected with a Hitachi SU3500 Scanning Electron Microscope (SEM) in the Colorado Shared Instrumentation in Nanofabrication and Characterization (COSINC) with 10.0 kV accelerating voltage, and a working distance of 5.0-9.0 mm. Many, but not all of the modern grain sites targeted using the electron microprobe were revisited using the SEM. The elemental compositions of the Green River Formation (VC-18-24) sample were confirmed via point analysis using an Oxford Instruments energy dispersive X-ray spectrometer (EDS) in tandem with Hitachi SU3500 Scanning Electron Microscope. EDS data was analyzed with AZtec nanoanalysis software.

X-ray Florescence (XRF) and Sulfur K-edge Absorption Spectroscopy (XAS)

X-ray fluorescence (XRF) mapping and x-ray absorption spectroscopy (XAS) were performed at Stanford Synchrotron Radiation Lightsource (SSRL) located in Menlo Park, California at beamline 14-3b. Bridger Bay Samples (GSL002 & GSL003) and Green River Sample (VC-18-24 were placed on a rotating stage within the experimental station hutch, and flushed with helium. XRF element maps were created using ~5x5 μm beam size to locate the distribution of silica, magnesium, and sulfur. Multiple coarse area maps were created on all samples and fine area maps were created for targeted grains, and grain revisits. Sulfur K-edge absorption spectroscopy point analysis (spot area of ~5x5 μm), was used for distinction of sulfur species from GSL and Green River samples. Determination of sulfur species was established by comparison of XAS spectral peaks with other studies employing similar sulfur K-edge absorption methodologies (Prang et al., 1999; Franz et al., 2007; Debret et al., 2017).

Image Analysis

The electron microprobe maps were analyzed for elemental zonal coincidence. Elemental ratios were determined using the open source image processing program, ImageJ with the ratio plus plugin.[2]XRF image maps were processed using the application, Sam's Microprobe Analysis Kit (SMAK)[3]. Analysis of Sulfur K-edge XAS was processed using the application, Sam's Interface for XAS Package (SIXPACK)[4].

Mapping

Spatial distribution of modern ooid deposits in the GSL photic zone was determined in ArcGIS. By first georeferencing a map produced by Eardley (1938) detailing sedimentary lithologies at the GSL. Ooid distribution from this map was converted to shapefile, and rasterized. Bathymetric profile of GSL was obtained via Hydroshare[5], was rasterized. Raster math was performed in order to determine the coincidence of ooid facies within the GSL photic zone, assumed to be at one meter depth of the lake surface. This map can be found as a supplement at the end of the text.

[2]Image J ratio plus plugin https://imagej.nih.gov/ij/plugins/ratio-plus.html

[3]Application for XRF image processing https://www.sams-xrays.com/smak

[4] Application for XAS data processing: https://www.sams-xrays.com/sixpack

[5]Tarboton, D. (2017). Great Salt Lake Bathymetry, HydroShare, http://www.hydroshare.org/resource/582060f00f6b443bb26e896426d9f62a

RESULTS

Modern GSL Ooids

Electron microprobe maps were compared to fabric structure with SEM backscatter images and transmitted light microscope images. Transmitted light images were found to give little indication of mineral composition within grain fabric. It was observed that zones of calcium and magnesium were found ubiquitously in all grains from all modern ooid samples. Analysis of zones of magnesium and silica coincided confirming Mg-silicate phase for all sample locations. The Mg-silicate phase was found distributed in isolated pockets, encompassed by areas dominated by calcium, and in many instances truncated by an accreted carbonate lamination. (see figure 5-A&B). A range of aragonite crystal sizes (see figure 5-B,11-C&D) make up the radial banding in the grain fabric. Distribution of Ca and Mg maps did not appear to overlap, except for in small areas in some but not all the grains. The methods used did not permit the determination of whether this phase is dolomite or a calcite containing high levels of Mg. Those zones containing both Ca and Mg were found in small enclaves no larger than 5 μm across situated: 1) in between aragonite and Mg-silicate phases or 2) completely surrounded by aragonite (see red arrows in figure 5-E).

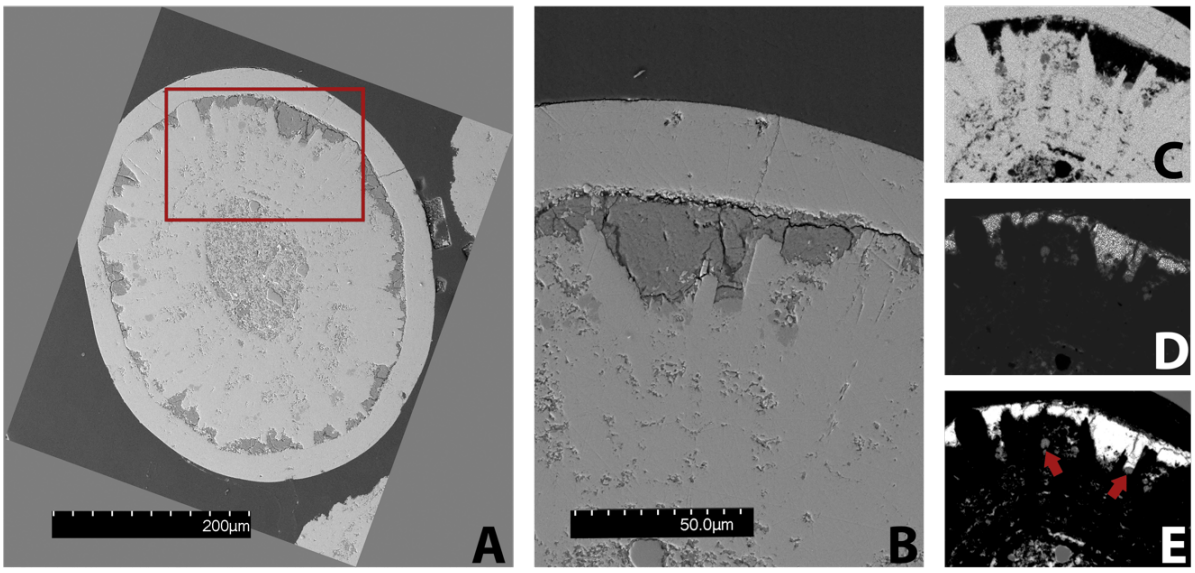

FIG. 5— Scanning Electron Microscope **(**SEM) and Electron Microprobe element maps for sample from Bridger Bay (GSL002- grain site 1) **A)** SEM image of entire ooid grain displaying radial banding fabric and accreted outer lamination. **B)** Detailed SEM image of crystal boundaries. Large euhedral aragonite crystals are arranged radially. **Images C-E)** Electron Microprobe maps. Lighter tones designate zones of element presence, darker tones indicate absence. Intermediate grey designates variable concentration. **C)** Calcium within cortex fabric **D)** Ratio map of Silica and Magnesium. **E)** Ratio map of Magnesium and Calcium. Red arrows point to enclaves of elemental coincidence.

Synchrotron K-edge XAS data revealed multiple sulfur species contained within grain fabrics in both modern and ancient samples. Spectral peaks (see figure 6) likely correspond with elemental sulfur at 2472.7 eV and carbonate associated sulfate (CAS) at 2482.6 eV. Synchrotron XRF mapping corroborated grains containing zones composed of both magnesium and silica from a site that had previously been mapped using the electron microprobe in the Bridger Bay ooid samples. Using this method, magnesium imaged at a lower resolution, but was found to correspond with

locations of concentrated silica (see figure 5-E). Signals of elemental sulfur (S_0), (see figure 7-B). were found concentrated coinciding within zones of magnesium and silica, whereas the CAS zones occurred in lower concentration pervasively across the entire aragonitic portion of the grain structure (See figure 7-C).

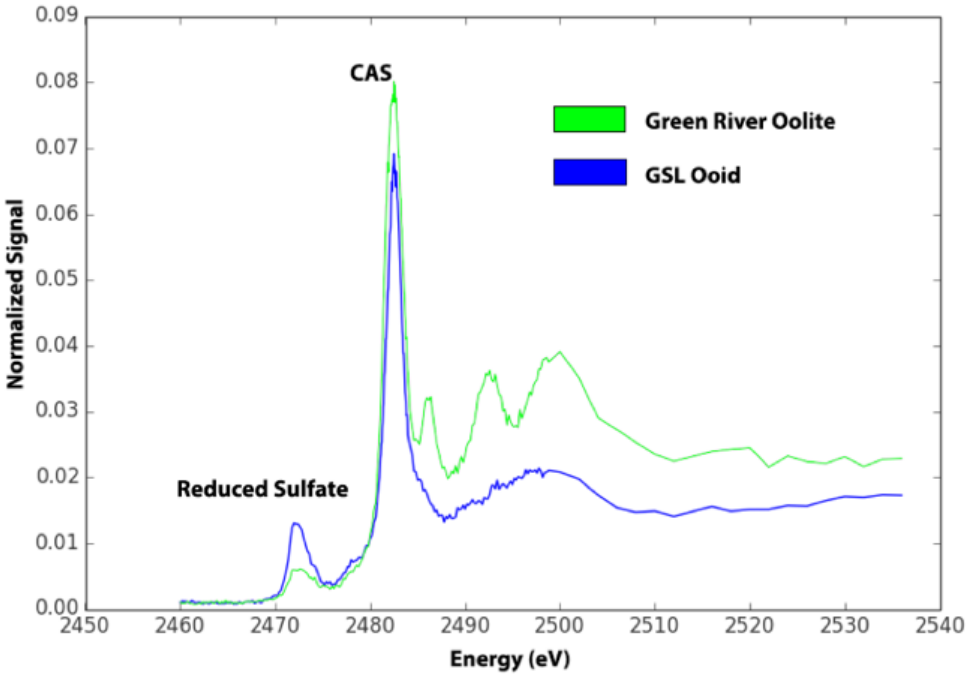

FIG. 6. — Sulfur K-edge absorption spectroscopy for modern ooid sample (GSL002) in blue, and ancient Green River Formation oolite sample (VC-18-24) in green. GSL ooid spectral peaks (blue) are identified as elemental sulfur (S_0) at 2472.7 eV and carbonate associated sulfate (CAS) at 2482.6 eV, and subsequently mapped in targeted grains using XRF while Green River oolite spectral peaks (green) were identified as pyrite (FeS_2) and carbonate associated sulfate (CAS) at 2482.6 eV.

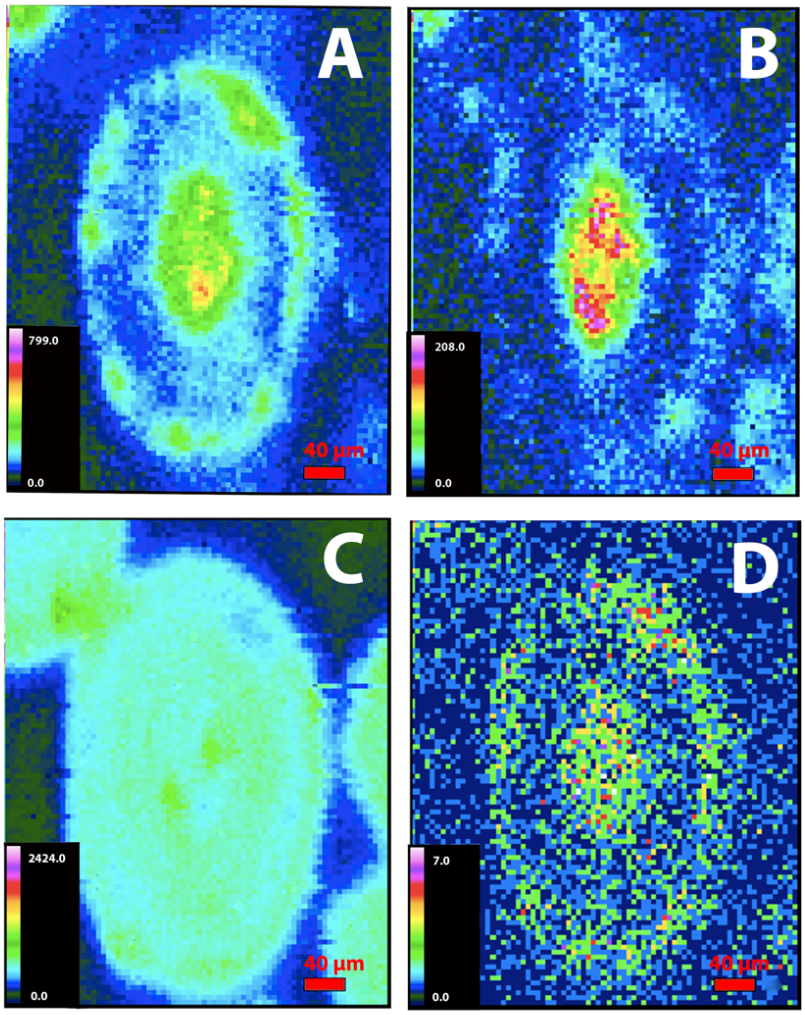

FIG. 7—Synchrotron X-ray fluorescence (XRF) maps of modern ooid grain from Bridger Bay (Sample GSL_002, Grain site 1). **A)** Silica map **B)** Elemental Sulfur (S_0) mapped at spectral peak 2472.7 eV **C)** Carbonate Associated Sulfur (CAS) mapped at spectral peak 2482.6 eV **D)** Magnesium registers at a lower resolution however appears to concentrate in cortical zones with Mg-silicate.

Ancient Green River Formation Oolite

Observations from EDS point analysis and XRF maps of the Green River Formation sample show that an 8 mm wide band grains contained on the thin section slide are silicified. Initial SEM backscatter images offer few grains within the Green River oolite sample that contain compositionally distinct dark zones or fabric structures comparable to those found in the modern GSL samples. Grains containing darker areas (see figure 8), where Mg-Si would be expected were not found as EDS and XRF spectral data demonstrated that these areas are silica dominated. White spots interspersed throughout the grain were found to be pyrite (FeS_2). XAS spectra for pyrite (Debret et al., 2017) are consistent with the data collected using the EDS. However, the modern ooids XRF maps spots throughout the grain fabric (see figure 9-B). It is inconclusive whether Mg-silicate is preserved in grain fabrics from in the Green river oolite.

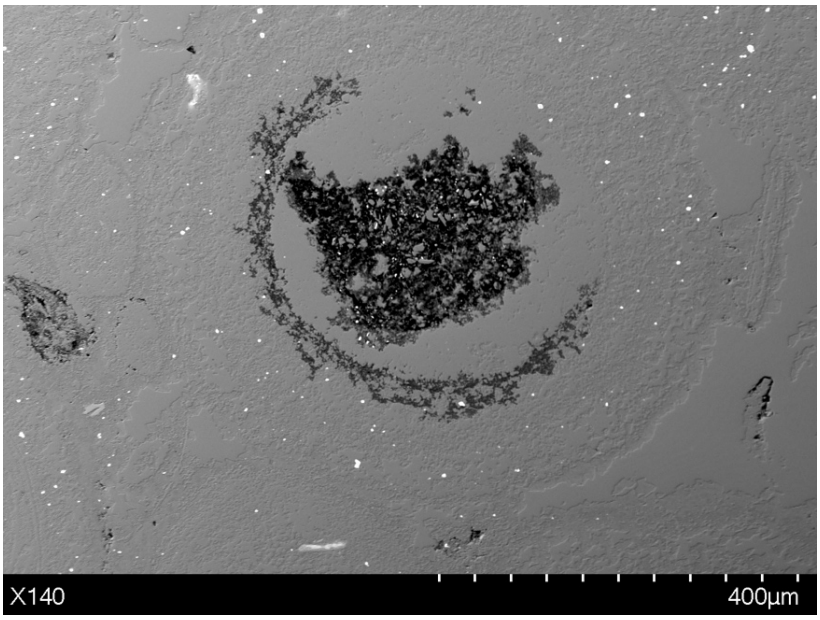

FIG. 8—SEM image of a grain in the Green River Formation oolite. EDS spectra of the partial concentric ring of dark area in the grain fabric did not indicate zones of Mg-Silicate. White spots were detected to be pyrite (FeS_2), however do not appear to coincide with features in the grain fabric.

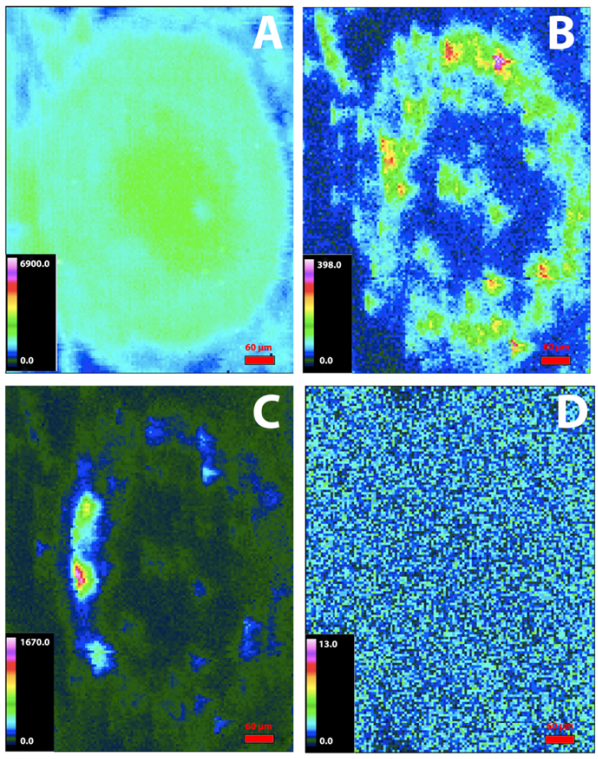

FIG. 9— Synchrotron X-ray fluorescence (XRF) maps of Eocene aged Green River Formation oolite (Sample VC-18-24) **A)** Silica map suggests that the entire grain has silicified. **B)** Reduced sulfur mapped at spectral species peak 2472 eV showing 'hot-spots' throughout the grain fabric **C)** Carbonate Associated Sulfur (CAS) mapped at spectral species peak 2482.6 eV **D)** Magnesium signal is not detected to coincide with features in the grain fabric.

DISCUSSION

Modern GSL Ooids

Areas of large aragonite crystals growing and protruding into areas of Mg-silicate (see figures 10 & 11) are exhibited across many of the modern ooid grain maps. The apparent unconformable arrangement of these aragonite crystals through the tangential laminations and growing into the host Mg-Si zone is characteristic of automorphic penetration; where one mineral clearly cuts across one mineral boundary into another (Boggs, 2009). The unique features of each cortical fabric structure in GSL ooids may represent grains in varying stages of the neomorphism and diagenesis; along with the dynamic interplay between abrasion and precipitation. Precipitation of additional laminations is likely to occur when ooid grains are located in the lake photic zone, where according to Pace et al. (2016), photosynthetic cyanobacteria increase the local lake water, alkalinity favoring the nucleation of the Mg-silicate phase. During this stage, heterotrophic bacteria colonize the grain surface. XRF maps indicate that zones of magnesium silicate coincide with concentrations of elemental sulfur. Here, elemental sulfur is likely a residual digestive intermediate product from the heterotrophic sulfate reducing bacteria. In accordance with the conceptual model proposed by Pace et. al (2016), these 'hot spots' of sulfur reduction are the probable loci for aragonite precipitation.

One possible early stage grain examined from Bridger Bay grain shows deformation of laminar structures, with an apparent 'puncture' from the formation of large aragonite needles (see red arrow in figure 11-C). It is commonplace for a clay matrix to be replaced by carbonate minerals; however, it is cautioned that determining paragenetic sequences in replacement events can be complex as mineral replacement can occur in multiple stages, and can often times involve phase reversals (Boggs, 2009). Similar neomorphic sequences have been noted in some laminated freshwater travertine and stromatolites (Love & Chafetz, 1988; Chafetz & Buczynski, 1992; Freytet & Verrecchia, 1999). In these examples, organic crusts initially build upon previously precipitated carbonates. As the sequence continues, the organic crust becomes engulfed by sparry calcium carbonate crystals. In the final stage, the organic crust becomes overcome by the carbonate crystal lattice, leaving little evidence of the organic lamination. Within GSL ooids, aragonite appears to encroach and ultimately occlude isolated pockets of Mg-silicate.

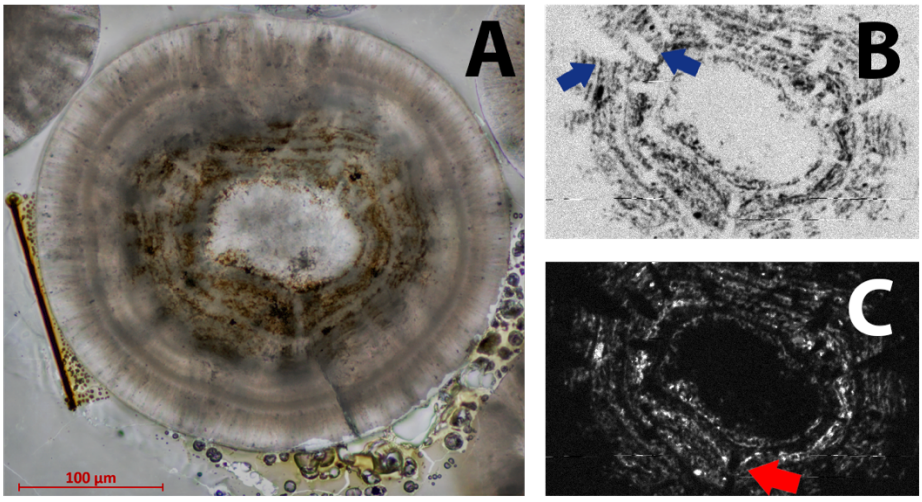

FIG. 10— Ooid grain from Bridger Bay (sample BB5 grain map 11) **A)** Transmitted light microscope image **B)** Microprobe imaging of Ca, large aragonite (blue arrows) crystals penetrate through many laminar accretions. **C)** Mg-Ca ratio map with apparent rupture and distortion of the laminar fabric by a large aragonite needle.

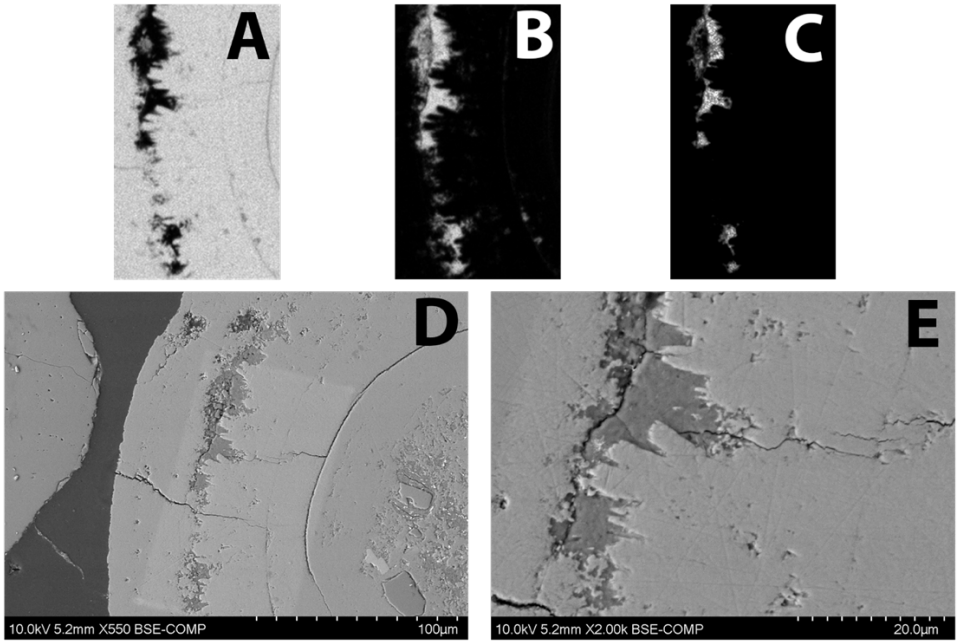

FIG. 11— Bridger Bay (sample GSL002- grain site 6) Images **A-B :** Electron Microprobe element maps **A)** Calcium map **B)** Magnesium map **C)** Mg-Ca ratio map ratio map. Images **D)** & **E)** SEM detail images showing euhedral aragonite crystals intruding into Mg-silicate phase.

It is difficult to position the Mg/Ca phase within the paragenetic sequence due to the infrequency in grain fabrics, its position in small isolated enclaves either completely enveloped by aragonite or situated between aragonite and Mg/Si phases, and the polished thin section surface disguises crystalline structure. In the situation that the Mg/Ca mineral is dolomite and forms as a tertiary phase, that is after Mg-Silicate and aragonite, it would be expected that the growth of rhombic crystals to extend outward from the observed enclaved zones (see figure 12). When aragonite is the host mineral in replacement with dolomite, dolomite will nucleate non-epitaxially, that is, the

fabric structure will be preserved but retain the original crystallographic orientation of the aragonite (Sibley, 1978). Acid etching on the polished surface and further SEM imaging may bring further clarity to this phase.

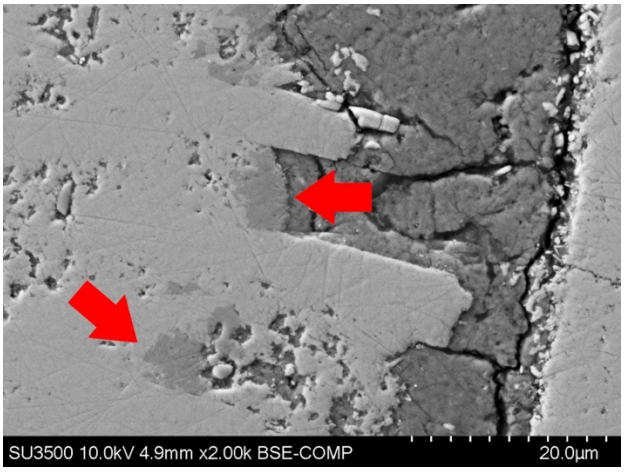

FIG. 12— Bridger Bay (GSL002- grain site 1) SEM detail. Red arrows point to Mg/Ca zones.

Ancient Green River Formation Oolite

Partial silicification of the Green River Fm. sample may be explained by the variable depositional conditions for diagenesis of these grains. High influx of dissolved silicic material, likely volcanic in origin associated with active volcanism in the Absaroka and Challis provinces during Eocene time (Smith et al., 2003), contributed to the partial silicification of the ooids in these facies. In spite of the silicified band, grains were examined in both silicified and non-silicified portions of the sample, as other mineral phases may or may not have been preserved between the portions. Minerals, mainly stevensite, containing Mg & Si were found preserved in the same Eocene aged oolite from the Uinta Basin, Mg-silicate was not detected in the grain fabrics from sampled sites. Additional assessment from other samples from this location will need tobe performed to ensure that this phase is completely absent.

'Hot spot' concentrations of reduced sulfate was found (see figure 9-B) preserved in grain fabric may indicate similar microbial meditated carbonate precipitation occurred during some point in the stratigraphic history of the ancient oolite; however, phase structures may be not be preserved as a result of diagenesis and silicification. Pyrite (FeS_2) was also confirmed and detected in these grains using XAS and EDS, although the placement of the mineral does not appear to coincide with these reduced sulfate concentrations nor features within grain fabric. The formation of pyrite in sediments is considered to be catalyzed by microbial reduction reactions (Thiel et al., 2019). In either case if the reduced sulfate concentrations and the pyrite minerals are linked or not, each are a reduced state of sulfur, indicating that microbial mediation may have played a role in the diagenetic process during the history of the oolite.

CONCLUSIONS

The development of radial bands in modern GSL ooids are found to be tandem products of both physical and biotic factors. The energy of the environment plays a physical role; i.e. ooids here are relatively stationary, lacking major agitation and abrasion, unlike the marine counterparts. Pace et al. (2016) laid out a conceptual model detailing the microbial role in the lithification of microbialites at the shores of the GSL. Using multiple methods of microscopy, it was determined that ooids at the GSL mineralize in a similar sequence. Aragonite crystals that make radial bands within cortex fabrics were found to intrude and ultimately engulf zones of Mg-silicate, similar to processes that form fabrics in freshwater travertines and stromatolites. The loci of nucleation of aragonite crystals was found to coincide with zones of Mg-silicate and concentrations of reduced sulfate, an intermediate product in microbial redox reactions. The finding of reduced sulfate in these zones carries the implication microbial mediation played a role in development of radial texture within ooids. This suggestion contradicts previous speculation that radial banding was a result of depositional processes, rather than diagenetic. It is suspected that similar mineralization and microbial mediation processes occur in ooids from analogous paleo-settings, however further investigations are required to support any claim.

REFERENCES

Awramik S.M., & Buchheim, H. P. (2015) Giant stromatolites of the Eocene Green River Formation (Colorado, USA). *Geology*; 43 (8): 691–694.

Bathurst, R. G. C. (1975) Carbonate Sediments and their Diagenesis *Elsevier Science Publ. Co., New York* p. 658

Beukes N.J. (1983) Ooids and Oolites of the Proterophytic Boomplaas Formation, Transvaal Supergroup, Griqualand West, South Africa*. In: Peryt T.M. (eds) Coated Grains.* Springer, Berlin, Heidelberg

Boggs, S. Jr. (2009) Petrology of Sedimentary Rocks. *Cambridge University Press*. p. 296-298

Bouton, A., Pace, A.,Vennin, E., Bourillot, R. *et al.* (2016) Linking the distribution of microbial deposits from the Great Salt Lake (Utah , USA) to tectonic and climatic processes. *Biogeosciences Discussions.* DOI: 10.5194/bg-2015-647

Carroll A. R, & Bohacs, K. M, (1999) Stratigraphic classification of ancient lakes: Balancing tectonic and climatic controls. *GEOLOGY* vol. 27; no. 2; 99–102.

Chafetz, H. & Buczynski, (1992) Bacterially Induced Lithification of Microbial Mats *PALAIOS*, V. 7, p. 277-293

Cooley S. & Pederson J. (2012) Surficial Geology of the Oneida Narrows Area, Caribou and Franklin Counties Idaho. *Technical Report 12-6 v*ia Idaho Geologic Survey.

Debret, B., Andreani, M., Delacour, A., Rouméjon, S., Trcera, N., & Williams, H. (2017) Assessing sulfur redox state and distribution in abyssal serpentinites using XANES spectroscopy *Earth and Planetary Science Letter*s 466 (2017) 1–11

Deocampo, D. (2010) The Geochemistry of Continental Carbonates. *Developments in Sedimentology*, vol 62. p.12.

Eardley, A. J, (1938) Sediments of Great Salt Lake, Utah. *Bulletin of American Association of Petroleum Geologists.* Vol. 22; no.10; 1359-1387.

Franz, B., Lichtenberg, H., Hormes, J., Modrow, H., Dahl, C., & Prang, A. (2007) Utilization of solid 'elemental' sulfur by the phototrophic purple sulfur bacterium Allochromatium vinosum: a sulfur K-edge X-ray absorption spectroscopy study *Microbiology* 153, 1268–1274

Freytet, P, & Verrecchia, E.P. (1999) Calcitic radial palisadic fabric in freshwater stromatolites: diagenetic and recrystallized feature or physicochemical sinter crust? *Sedimentary Geology*, vol. 126 p. 97-102

Ingalls, M., Frantz, C. M., Snell, K. E., & Trower E.J. (in press) Carbonate facies-specific stable isotope data record climate hydrology, and microbial communities in the Great Salt Lake. *Geobiology*;. doi: 10.1111/gbi.12386

Love, K, & Chafetz, H. (1988) Diagenesis of Laminated Travertine Crusts, Arbuckle Mountains, Oklahoma. *Journal of Sedimentary Petrology* Vol. 58 no.3 p.441-445

Jones, B. F. (1986) Clay mineral diagenesis in lacustrine settings. *In: Mumpton, F. A. (ed.) Studies in Diagenesis.* United States Geological Survey, Reston, VA, Bulletins, 1578, 291–300.

Jones, B.F., Naftz, D.L., Spencer, R.J. & Oviatt, C.G. (2009) Geochemical Evolution of Great Salt Lake, Utah, USA. *Aquat Geochem* 15**,** 95–121. https://doi.org/10.1007/s10498-008-9047-y

Kahle, C. F, (1974) Ooids from Great Salt Lake, Utah, as an analogue for the genesis and diagenesis of ooids in marine limestones*. Journal of Sedimentary Research.* Vol 44 (1), 30–39.

`

Medwedeff, D. A., & Wilkinson, B.H. (1983) Cortical fabrics in calcite and aragonite ooids *Coated grains*. *Springer, Berlin, Heidelberg,* 109-115

McGuire, K. M (2014). Comparative Sedimentology of Lake Bonneville and the Great Salt Lake *BYU Scholars Archive. All Theses and Dissertations*. 4022.

Pace, A., Bourillot, R., Bouton, A., Vennin, E Galaup, S., *et al.* (2016). Microbial and diagenetic steps leading to the mineralisation of Great Salt Lake microbialites. *Scientific Reports.* **6**, 31495; doi: 10.1038/srep31495

Paradis, O.P., Corsetti, F.A., Bardsley, A., Xu, X., & Walker J.C. (2017) Radial ooids from Great Salt Lake (Utah) as paleoenvironmental archives: Insights from radiocarbon chronology and stable isotopes. *American Geophysical Union, Fall Meeting 2017,* abstract #EP12A-06

Prang A., Arzberger, I., Egemann, C., Modrow, H. Schumann, O., Trüper, H.G., Steudal, R., Dahl, C., & Hormes, J. (1999) In situ analysis of sulfur in the sulfur globules of phototrophic sulfur bacteria by X-ray absorption near edge spectroscopy *Biochimica et Biophysica Acta* 1428: 446-454.

Richter D.K. (1983) Calcareous Ooids: A Synopsis. *In: Peryt T.M. (eds) Coated Grains*. Springer, Berlin, Heidelberg

Reimer, T.O., 1975. Paleogeographic significance of the oldest known oolite pebbles in the Archaean Swaziland Supergroup (South Africa). *Sediment. Geol*.,14: 123--133.

Rey, K. A., 2012, Insights into the early transgressive history of Lake Bonneville from stratigraphic investigation of Pilot Valley, UT/NV, USA: *Thesis, Brigham Young University.*

Sibley, D. (1978) Dolomite textures. In: *Sedimentology. Encyclopedia of Earth Science*. Springer, Berlin, Heidelberg

Smith, E.M., Singer, B., & Carroll, A. (2003) 40Ar/39Ar geochronology of the Eocene Green River Formation, Wyoming. *GSA Bulletin*. 115 (5): 549–565.

Spencer, R., Baedecker, M.J., Eugster H.P., Forester, R.M., Goldhaber, M.B., Jones B.F., Kelts, K., Mckenzie, J., Madsen, D.B., Rettig, S.L., Rubin, M., & Bowser, C.J. (1984) Great Salt Lake, and precursors, Utah: The last 30,000 years. *Contr. Mineral. and Petrol.* 86**,** 321–334. https://doi.org/10.1007/BF01187137

Tettenhorst, R. & Moore, G. E. Jr. (1978). Stevensite Oolites from the Green River Formation of Central Utah. *J. Sediment*. *Res*. 48, 587–594

Thiel, J., Byrne, J.M., Kappler, A., Schink, B., & Pester, M. (2019) Pyrite formation from FeS and H_2S is mediated through microbial redox activity *Proceedings of the National Academy of Sciences* 116 (14) 6897-6902; DOI: 10.1073/pnas.1814412116

Trower, E.J., Cantine, M.D., Gomes, M.L., Grotzinger, J.P., Knoll, A.H., Lamb, M. P., Lingappa, U., O'Reilly, S.S., Present, T.M., Stein, N., Strauss, J. V., & Fischer, W.W. (2018). Active Ooid Growth Driven by Sediment Transport in a High-Energy Shoal, Little Ambergris Cay, Turks and Caicos Islands. *Journal of Sedimentary Research* 88 (9): 1132–1151.

Trower, L. What Controls Ooid Grain Size? (2015) *American Geophysical Union, Fall Meeting 2015,* abstract id. EP13C-0

Trower, E.J, Lamb, M.P, & Fischer, W.W. (2017) Experimental evidence that ooid size reflects a dynamic equilibrium between rapid precipitation and abrasion rates. *Earth and Planetary Science Letters* 468: p112–118

Trower, L. (2019) Cortical Stratigraphy of Ooids from Great Salt Lake, UT *American Geophysical Union, Fall Meeting 2019*, abstact id. PP41C-1566

Wright, P. (2012) Lacustrine carbonates in rift settings: the interaction of volcanic and microbial processes on carbonate deposition**.** *Geological Society, London, Special Publications***,** 370, 39-47, 26

SUPPLEMENTAL INFORMATION

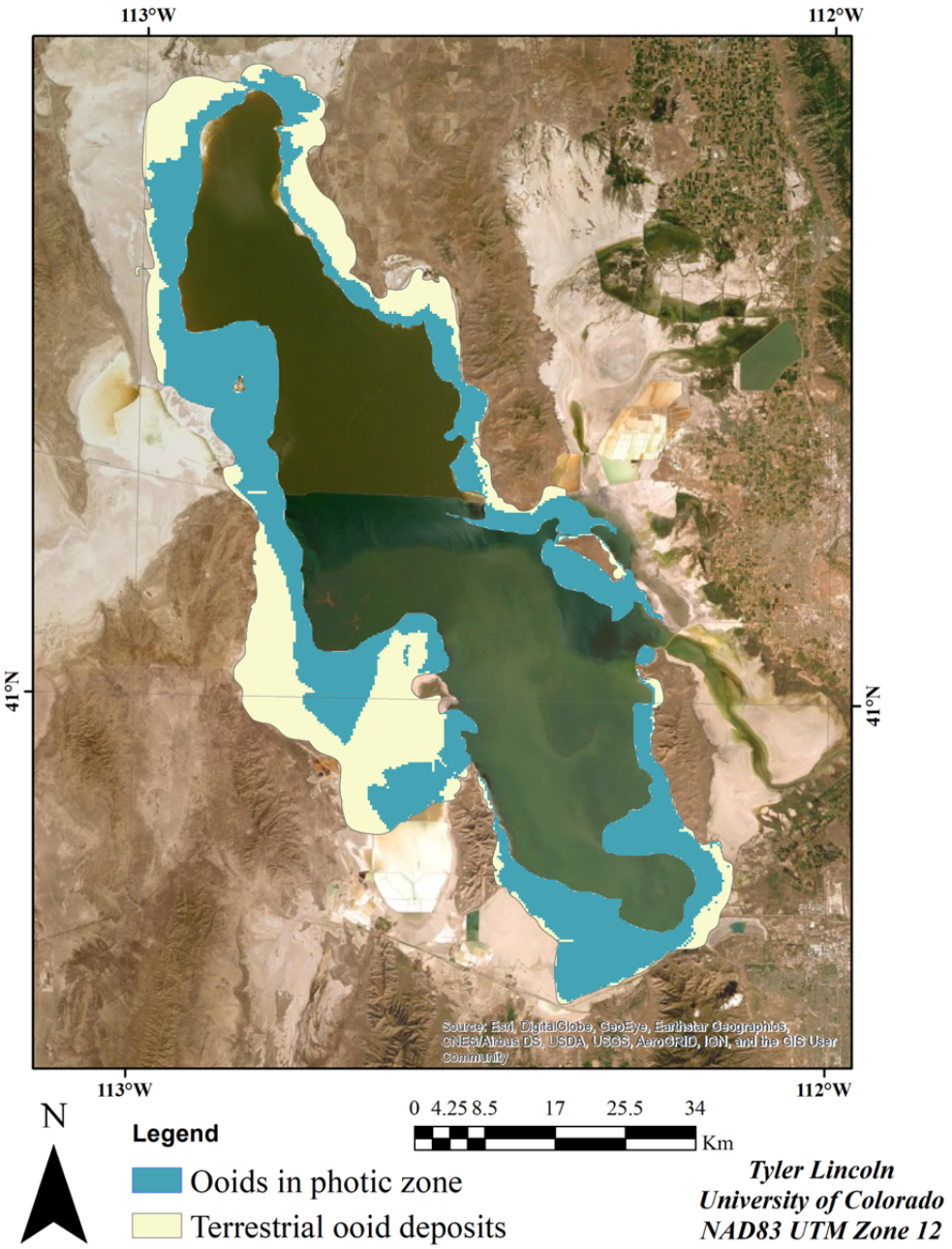

Supplemental Map 1: Produced in ArcGIS shows the coincidence of ooid sand deposits with the photic zone of the lake (1-meter depth of the lake surface).